The AAPS Journal, Vol. 13, No. 3, September 2011 (© 2011)
DOI: 10.1208/s12248-011-9288-3

Research Article

Characterization of Microchannels Created by Metal Microneedles: Formation and Closure

Haripriya Kalluri,[1] Chandra Sekhar Kolli,[2] and Ajay K. Banga[1,3]

Received 27 January 2011; accepted 22 June 2011; published online 6 July 2011

Abstract. Transdermal delivery of therapeutic agents for cosmetic therapy is limited to small and lipophilic molecules by the stratum corneum barrier. Microneedle technology overcomes this barrier and offers a minimally invasive and painless route of administration. DermaRoller®, a commercially available handheld device, has metal microneedles embedded on its surface which offers a means of microporation. We have characterized the microneedles and the microchannels created by these microneedles in a hairless rat model, using models with 370 and 770 μm long microneedles. Scanning electron microscopy was employed to study the geometry and dimensions of the metal microneedles. Dye binding studies, histological sectioning, and confocal microscopy were performed to characterize the created microchannels. Recovery of skin barrier function after poration was studied via transepidermal water loss (TEWL) measurements, and direct observation of the pore closure process was investigated via calcein imaging. Characterization studies indicate that 770 μm long metal microneedles with an average base width of 140 μm and a sharp tip with a radius of 4 μm effectively created microchannels in the skin with an average depth of 152.5±9.6 μm and a surface diameter of 70.7±9.9 μm. TEWL measurements indicated that skin regains it barrier function around 4 to 5 h after poration, for both 370 and 770 μm microneedles. However, direct observation of pore closure, by calcein imaging, indicated that pores closed by 12 h for 370 μm microneedles and by 18 h for 770 μm microneedles. Pore closure can be further delayed significantly under occluded conditions.

KEY WORDS: microneedles; microporation; pore closure; skin; transdermal delivery.

INTRODUCTION

Stratum corneum (SC), the outermost layer of the skin, obstructs foreign particles as well as hydrophilic compounds from entering the body. Several enhancement methods such as intraepidermal administration, iontophoresis, ultrasound, electroporation, chemical enhancers, and microneedles (MN) have been employed to overcome this barrier (1–10) and new minimally invasive techniques are continually being investigated. While chemical enhancers have been widely investigated for enhancing drug permeation levels, they tend to disrupt the lipid bilayers of the stratum corneum. Alternatively, physical enhancement methods have been used.

Microneedle technology offers a minimally invasive and painless route of drug administration (11). This technology, which is currently being investigated by several research groups and companies, involves the creation of channels in the skin with micron-sized dimensions, thereby enabling the delivery of a broad range of therapeutic molecules including proteins which would not otherwise cross intact skin. Since microneedles have micron-sized dimensions, microporation and drug delivery is relatively painless (12,13) and results in no significant skin damage. Possibility of irritation and infection is also minimal, as investigated and reported by Donnelly *et al.* (14). Further, according to a recent study, the perception of this technology in patients and health care providers is positive (15). Microneedle arrays can be fabricated from a wide range of materials such as silicon, glass, metals, and polymers and can be further incorporated into a patch or a device. DermaRoller® (DR), a commercially available cosmetic handheld device, equipped with microneedles intended to be rolled on the skin, offers a means for breaching the stratum corneum barrier. It is currently used in the cosmetic industry to treat several skin conditions such as pigmentation problems, wrinkles, acne, burn-related scars, big pores, and is also a part of collagen induction therapy (16–19).

These devices are available in varying microneedle lengths (ranging from 0.13 to 1.5 mm), each specific for the nature of treatment it is being employed for. Recent studies with different types and lengths of microneedles have helped in proposing an ideal range of microneedle lengths for optimal, painless drug delivery. Henry *et al.* (20) reported an increase in human skin permeability up to a magnitude of 4 orders with the use of 150 μm long MN, which is on the lower side of the length scale. Microneedle lengths up to 750 μm have been reported to be painless upon administration

[1] Department of Pharmaceutical Sciences, College of Pharmacy and Health Sciences, Mercer University, 3001 Mercer University Drive, Atlanta, Georgia 30341, USA.
[2] California Northstate College of Pharmacy, Rancho Cordova, California 95670, USA.
[3] To whom correspondence should be addressed. (e-mail: banga_ak@mercer.edu)

(11,13). In this series of experiments, we have focused on a DermaRoller® model with 770 μm long microneedles and characterized the microchannels created by the metal microneedles which can enhance delivery. For the first time, we have reported the dimensions of the microchannels created by these metal microneedles and the time taken for their closure, in a hairless rat model. Shorter microneedles, 370 μm in length (DR), were also employed to study the effect of microneedle length on pore closure. The effect of microneedle length on pore closure has not been previously reported to our knowledge.

MATERIALS AND METHODS

Materials

Two DermaRoller® microneedle devices with 370 and 770 μm long microneedles were employed for these studies. Both models are equipped with 192 stainless steel microneedles stacked in eight rows, and the assembly is about 20 mm wide (provided by DERMAROLLER S.A.R. L., Friesenheim, France). Fluoresoft (0.35%)® used in confocal and calcein imaging studies was obtained from Holles Laboratories Inc., Cohasset, MA, USA. Methylene blue dye, used in the dye binding studies, was obtained from Eastman Kodak Co, Rochester, NY, USA.

Male hairless rats, the animal model used for these studies, were obtained from Charles River Laboratories (Wilmington, MA, USA) and were housed in the Mercer University animal facility until use. All the animal studies were reviewed and approved by the Mercer University Institutional Animal Care and Use Committee.

Methods

Scanning Electron Microscopy

The dimensions and geometry of metal microneedles on the DermaRoller® devices were studied using a Topcon (DS 130F) field emission scanning electron microscope (SEM). The head of the device was detached from the holder and placed in an Emscope SC500 sputter coater with gold target. The system was purged with Argon gas, and an approximate 12 nm thick layer of gold was sputter coated onto the sample. The sample was then placed in a field emission SEM at an accelerating voltage of 10 kV. Gold is a rich source of secondary electrons and the gold coating keeps the sample conductive and connected to the ground, aiding as a pathway for the electrons being bombarded on the sample by the laser beam. Secondary ion images were collected at different magnifications to study the dimensions and geometry of the needles.

Characterization of Microchannels Created by Metal Microneedles (770 μm)

Methylene blue staining was performed to check for creation of microchannels by the metal microneedles. Freshly excised full thickness skin was obtained by euthanizing hairless rats by carbon dioxide asphyxiation. Skin samples were placed flat on a stack of paper towels, and the desired treatment site was stretched with fingers before treatment with one pass of the device in order to overcome skin's inherent elastic nature which may hinder successful poration of microneedles and will also directly affect the depth to which microneedles can reach in the skin. Methylene blue dye (0.1%, *w*/*v*) was then applied for 1 min following which the site was cleaned with alcohol swabs and kimwipes. A 1 cm^2 area was measured and marked, and images were taken using a video microscope (ProScope HR). A similar procedure was repeated to check the number of microchannels created after treating the skin with 3×, 5×, 10×, and 15× passes of the device.

Histological sectioning was also performed to confirm creation of the microchannels. Excised full thickness hairless rat skin was treated with one pass of the device. A small area of the treated skin was cut and fixed in optical coherence tomography (OCT) compound medium. The blocks where instantly frozen using liquid nitrogen and were stored at −80° C until further analysis. Using a Leica CM1850 cryostat, 8 μm cryosections of the skin sample were cut and placed on a glass slide. Hematoxylin and eosin staining was performed to visualize the disruption of the stratum corneum at the sites where the microneedles penetrated the skin.

Confocal microscopy was then performed to characterize the dimensions of the created microchannels. Freshly excised full thickness skin was obtained and was treated with one pass of the device. The porated site was treated with 200 μL of 0.2 μm FluoSpheres® (Invitrogen™, Carlsbad, CA, USA) for ~1 min after which the site was blotted with kimwipes. A Zeiss Confocal laser microscope LSM410 (Goettinger, Germany) was employed at ×10 magnification and at an excitation wavelength of 488 nm. X–Z sectioning was performed to observe the permeation pattern of the fluorescent microparticles down the microchannels which would in turn indicate the depth of the created microchannels.

Assessment of Barrier Integrity as Indicated by Transepidermal Water Loss

Hairless rats were anesthetized using ketamine (70 mg/kg) and xylazine (10 mg/kg). A VapoMeter (Delfin Technologies Ltd, Kuopio, Finland) was used to measure the increase in transepidermal water loss (TEWL) after treatment with the device. The VapoMeter consists of sensors which measure the percent relative humidity and convert it to a value representative of TEWL. TEWL values were recorded as a function of number of passes of the device.

This technique was also employed to study the time taken by skin to regain its barrier function after poration. Both selected microneedling devices were employed to study the effect of microneedle length on time required for skin to regain its barrier function. An area on the abdomen was marked and base TEWL values were recorded which indicated intact skin. TEWL values were again recorded immediately after poration (five passes of DR) which served as controls, indicating perturbed skin barrier. TEWL values were further monitored continuously till they recovered to base values indicating recovery of skin barrier function. These studies were performed on three rats for each microneedle length, with readings taken from three sites on each rat. The data presented are an average (± SD) of the pattern seen for all the sites.

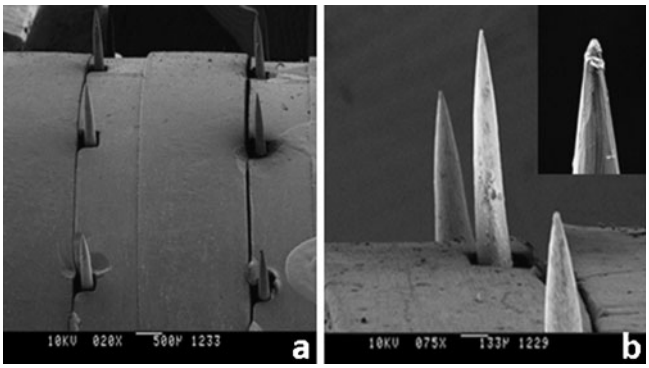

Fig. 1. SEM images of metal microneedles. **a** ×20 magnification; array of metal microneedles embedded in the head of the device; **b** ×75 magnification; *inset*: ×130 magnification of the tip of a single microneedle

Calcein Imaging to Study Pore Uniformity and Pore Closure

Calcein imaging studies were performed to study the uniformity of the created microchannels. Hairless rats were anesthetized; an area on the abdomen was slightly stretched and was treated with the DR. Calcein (Fluoresoft-0.35%®, Holles Laboratories, Inc., Cohasset, MA, USA), a fluorescent dye with excitation/emission wavelengths of 495/515 nm was applied to the treated site for ~1 min. After application, the site was wiped with kimwipes and alcohol swabs to remove the excess dye. A fluorescent image was taken that shows the two-dimensional distribution of fluorescent intensity in and around each pore. The imaging system used by Kolli and Banga (21) was employed for these studies. It comprises of a digital camera (Canon, USA) fitted with a macro lens attached in front with a 525 nm long pass filter. The obtained fluorescent images were then analyzed using Fluoropore software, an image analysis tool, to measure the relative skin permeability. The software first calibrates each image with set standards based on the quality of the image. Next, the microchannels are selected individually, and the software converts the calcein intensity in and around each pore, based on the pixel density, into a value called the pore permeability index (PPI) which is representative of calcein flux for each pore.

Calcein imaging was also employed as the main technique to directly observe the pore closure process in skin treated with microneedles. Microneedle treated sites were imaged, as described above, at different time points after poration to study the time taken for pore closure. Effect of microneedle length on pore closure was also investigated by performing similar studies with 370 μm sized, shorter microneedles as well.

RESULTS AND DISCUSSION

Traditionally, chemical agents such as esters, azones, cyclodextrins, etc. have been employed in formulations as a means to alter the barrier properties of the stratum corneum layer of skin and aid in better permeation of the active agent. These permeation enhancers tend to disrupt the lipid structure of the SC layer, thereby causing damage which takes a long recovery time (22). Physical enhancement techniques like iontophoresis, sonophoresis, and microdermabrasion overcome the stratum corneum barrier effectively. However, they have their own set of limitations. Application of iontophoresis for drug delivery is limited by the restriction on the size of the drug molecule can be administered by this technique (~12 kDa). On the other hand, sonophoresis and microdermabrasion techniques are limited by their large equipment size. Microneedle technology overcomes all these limitations by creating micron-sized channels in the skin which can deliver even microparticles into/across skin without any irreversible damage and irritation issues.

In this series of experiments, we characterized the DermaRoller®, a commercially available handheld device currently on the market for cosmetic applications, for use in topical and transdermal drug delivery. Scanning electron microscopy of both the DR models showed the conical shape of the microneedles embedded on the roller head (Fig. 1). The longer microneedles have an average length of 770±75.6 μm, base width of 137.5±7.3 μm, and a tip radius of ~4 μm, while the shorter microneedles have an average length of 376.4±8.9 μm and a base width of 118.8±6.7 μm, suggesting that these structures are comparable to the maltose microneedles which have are already been extensively characterized and employed for transdermal delivery of drugs (21,23,24).

Dye binding studies were performed with methylene blue dye to visualize the formation of microchannels by longer microneedles and robustness of the device for repeated applications. Metal microneedles effectively penetrated the stratum corneum barrier and created microchannels in the skin. The areas of skin breached by microneedles took up the methylene blue dye whereas the rest of the skin remained

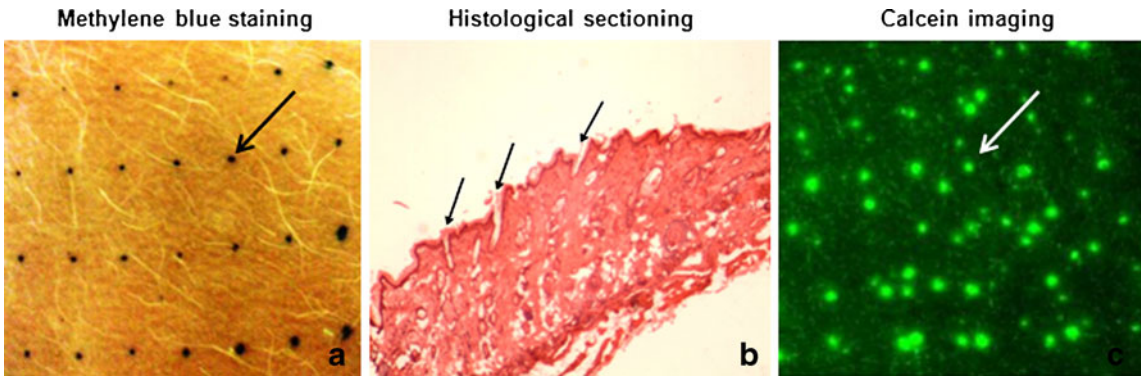

Fig. 2. Metal microneedles successfully created microchannels in skin as indicated by **a** methylene blue staining, **b** histological sectioning, and **c** calcein imaging studies. Each *arrow* indicates one single microchannel

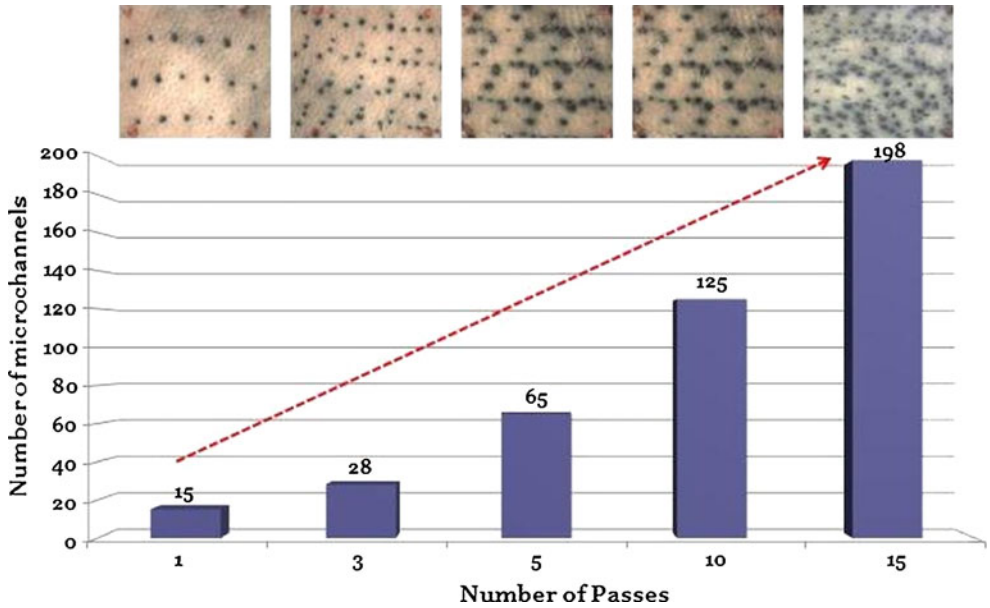

Fig. 3. DermaRoller® created microchannels in a reproducible manner. The number of microchannels increased as a function of number of passes

impermeable (Fig. 2a). The device created ~16 microchannels per square centimeter with an average surface diameter of ~70.7 ±9.9 μm. This pattern increased as a function of the number of passes of the device as can be seen in Fig. 3. A similar microporation pattern has been reported for the model with 370 μm needles as well which creates 250 microchannels/cm^2 after 15 passes (16). This is a very useful property allowing flexibility in treatment with the same instrument. Multiple treatments with the same device may be ideal for enhanced delivery for different drug candidates, and since the microneedles are made of metal, the device can be easily sterilized and reused. To confirm breach of the stratum corneum barrier, cryosections of the treated skin were prepared as previously discussed, and hematoxylin and eosin staining was performed. The microneedles penetrated the skin beyond the stratum corneum barrier as indicated by the arrows in Fig. 2b.

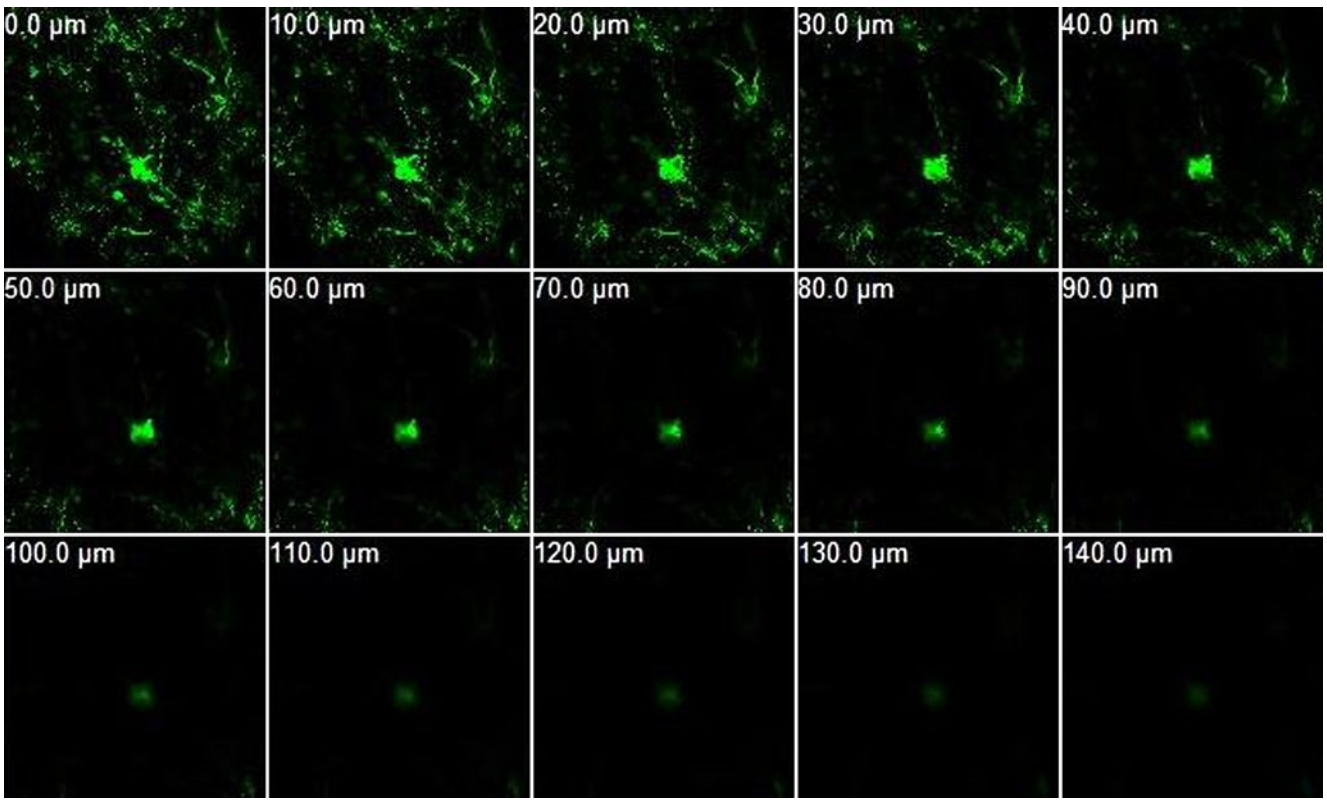

Fig. 4. Confocal microscopy with 0.2 μm sized FluoSpheres® to study the depth of the created microchannels. Permeation pattern indicated depth of microchannels to be ~140±20 μm

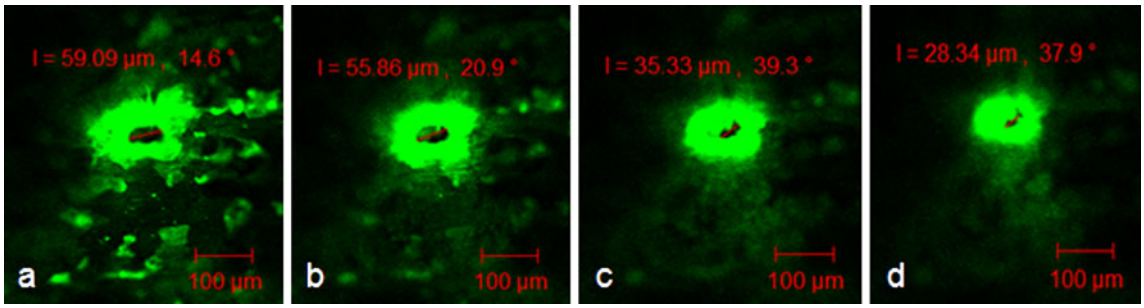

Fig. 5. Confocal images showing the diameter of a single microchannel at a depth of **a** 10 µm, **b** 20 µm, **c** 30 µm, and **d** 40 µm depth from the surface of the skin

Dimensions of the created microchannels were then investigated via confocal microscopy with micron-sized fluorescent particles. The permeation pattern of these microparticles along the microchannels would in turn indicate the depth of the created microchannels. The non-disrupted areas served as the control, and results revealed no fluorescence for the control area. In contrast, in the region of skin that was perturbed by the microneedles, FluoSpheres® migrated down, along the microchannels, to an average depth of about 152.5±9.6 µm (Fig. 4). Further, the diameter of the microchannels was also characterized as a function of the depth of penetration. The average diameter of the microchannels at the surface of the skin is about 70 µm. The surface diameter was also confirmed by analysis of methylene blue stained images using Screen Calipers, a digital measurement tool. The average diameter of the microchannels decreased as the depth of penetration increased (Fig. 5), which agrees with the conical shape of the microneedles. It is to be noted that microchannel depths are directly affected by skin's elasticity, application force, and person-to-person variability, and these aspects can be controlled for obtaining the desired microchannel depth.

While dye binding studies indicated the robustness of the device to create microchannels in a reproducible manner, uniformity of the created microchannels is desired as this will affect drug delivery. To assess this, calcein imaging was performed where drug and the fluorescent images were analyzed further to get a pore permeability value for each pore which is representative of calcein flux in and around each pore. Plotting a histogram of all the pore permeability values indicated the uniformity of the created pores (PPI 21; Fig. 6). This essentially implies that the created microchannels have similar surface dimensions, a feature that is desired for optimal delivery.

The degree of disruption of the skin barrier was also assessed by TEWL measurements. Skin, being an open system, has continual water loss from its surface. However, this water loss, termed the transepidermal water loss, is very minimal. When the stratum corneum barrier is disrupted, the amount of water loss from skin increases. Thus, a measurable difference from the baseline is indicative of disruption of the SC and is an indirect measure of increased permeability of the skin. Following treatment with 770 µm needles, TEWL values increased significantly and continued to increase as a function of the number of passes of the device. After 15 passes, TEWL increased from a base value of 10.23 to 28.55 g/m^2 h (Fig. 7). This confirms that the same device can be used for repeated applications to enhance drug delivery even further.

The created microchannels, however, would eventually close reducing drug delivery. Even though the DermaRoller® device has been used in cosmetic clinics extensively, the pore closure pattern for the microchannels created by these stainless steel microneedles has not been investigated. Therefore, following microporation, the time taken for skin to regain its barrier function and for complete pore closure was investigated by measuring the transepidermal water loss from treated sites and calcein imaging studies, respectively. The DermaRoller® model with 370 µm long microneedles was also employed for these studies to further understand the effect of microneedle length on pore closure kinetics.

Immediately following microporation, transepidermal water loss increased significantly for both microneedle lengths (370 and 770 µm) indicating disruption of the skin barrier. In a study by another group, treatment with increasing lengths of microneedles on DR devices resulted in increased transepidermal water loss indicating increased the degree of disruption of the barrier (25).

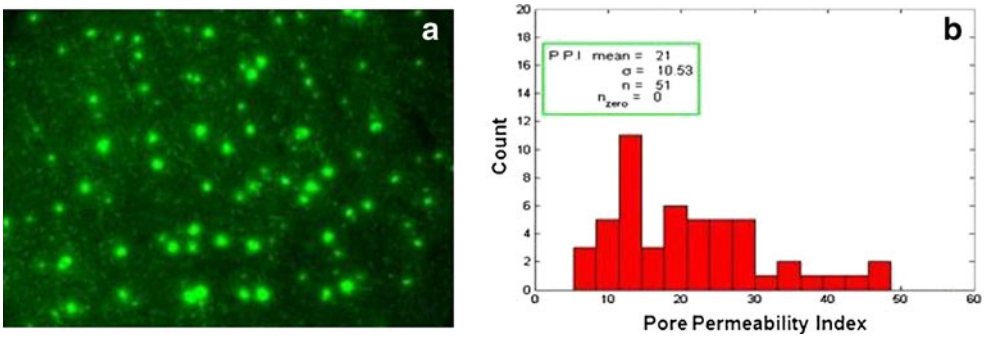

Fig. 6. Calcein imaging to check uniformity of microchannels. **a** A fluorescent image showing the created microchannels and **b** histogram; count of microchannels *vs.* pore permeability index (PPI) value; the mean PPI was found to be 21 which is indicative of the average calcein flux through the microchannels

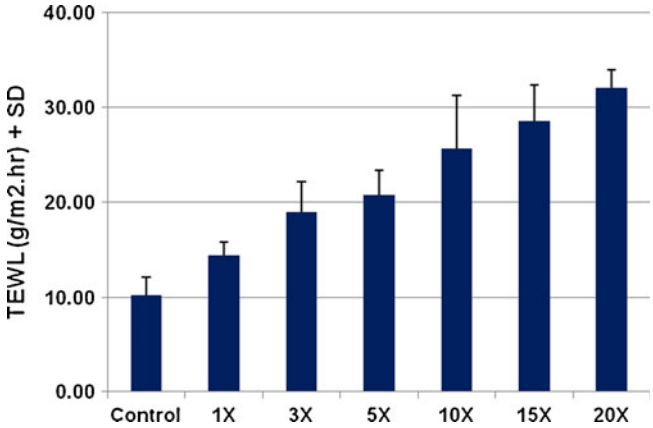

Fig. 7. Transepidermal water loss (TEWL) measurements were taken to study disruption of skin barrier after treatment with DermaRoller® (n=3). TEWL values increased as a function of the number of passes indicating increasing disruption of the skin barrier

This loss of water creates an imbalance in the skin which then triggers the skin healing process to restore the water gradient in skin. Continuous monitoring of this water loss over a period of time indicated that TEWL values decreased over a period of time and reached their base values around 4 to 5 h after poration, thus indicating recovery of skin barrier function (Fig. 8). The TEWL recovery time for both microneedle lengths was similar (around 4 to 5 h) indicating that microneedle length (370 *vs* 770 μm) did not have an effect on the time required for skin to regain its barrier function. Statistical analysis (t test) of recovery data for both microneedle lengths indicated no difference in the profiles. The observed TEWL recovery pattern differs from results from another study with DR series where TEWL reached its maximal value at 1 h after poration and eventually decreased around 2 h for all MN lengths (25). This restoration of barrier function, however, does not necessarily indicate complete pore closure where the superficial layers of skin (stratum corneum) have completely healed. From our understanding of the pore closure process from previous studies with soluble microneedles, we can safely conclude that even after restoration of the water gradient, delivery through skin can be enhanced until the time point when the superficial layers completely heal. Therefore, direct imaging studies appear to be more representative of the pore closure process as compared to TEWL data.

Calcein imaging studies were therefore performed for direct visualization of this pore closure process. Calcein dye used in these studies binds to only living cells which are exposed upon disruption of the skin barrier, thereby indicating presence or absence of pores. In skin sites treated with 770 μm long microneedles, complete pore closure did not occur until a much later point as compared to the TEWL recovery time. Pores closed completely by 18 h after poration (Fig. 9). Calcein imaging studies with 370 μm sized microneedles indicated that complete pore closure occurred by 12 h after poration (Fig. 10). While the observed, significantly shorter, time for closure of pores created by shorter microneedles is expected, it is interesting that microneedle length did not have an effect on barrier function recovery time, as monitored by TEWL. While microneedle length will directly affect the robustness of the microchannel creation process and their dimensions, it is also very important to consider this aspect for pore closure as it directly affects drug delivery. For example, drug delivery through skin treated with shorter microneedles may be significantly less as compared to that through longer needles due to the presence of open pores for a longer time.

The observed results are comparable to the pore closure pattern observed for microchannels created by soluble maltose microneedles (24). Microchannels created by 500 μm long soluble maltose microneedles have been reported to close within 15 h of poration under non-occluded conditions, as compared to 18 h by the metal microneedles of similar length. While there is not a significant difference in pore closure times for the tested soluble *vs* metal microneedles, the

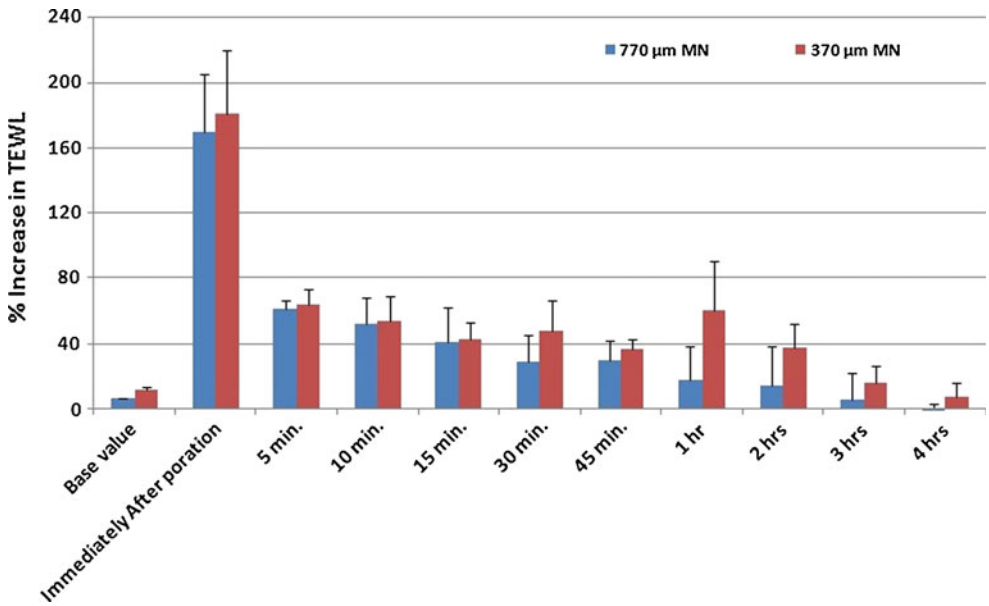

Fig. 8. Recovery of skin barrier function over time after treatment with five passes of the DR: 370 *vs* 770 μm sized microneedles (n=3 with nine sites for each study). TEWL values fell back to base values around 4 h after poration for both microneedle lengths indicating microneedle length did not have an effect on time required for skin to regain its barrier function

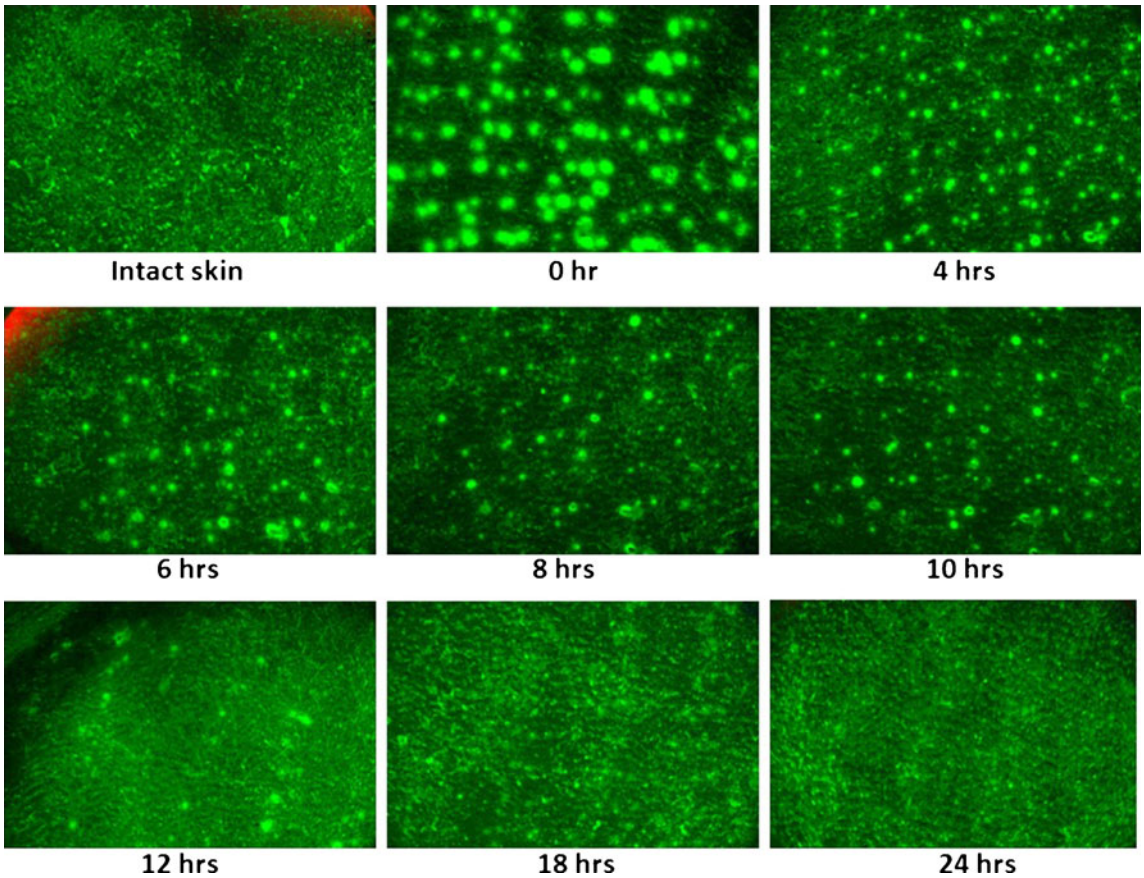

Fig. 9. Calcein imaging to study closure of pores created by 770 μm sized metal microneedles. Pores closed by 18 h, *in vivo*, indicating the reversible nature of skin microporation

effect of skin elasticity and other biomechanical aspects of skin are important aspects which need to be investigated further at a microscopic level as they may have direct implications on drug delivery. Coulman *et al.* reported that insertion of a 26G hypodermic needle (with a diameter of 450 μm) into skin resulted in a microchannel that is 50 times smaller in diameter (26). A similar pattern was observed in our studies as well where the soluble microneedles with base width of >200 μm resulted in microchannels with a surface diameter of only 60–70 μm (24). Badran *et al.* (25) performed

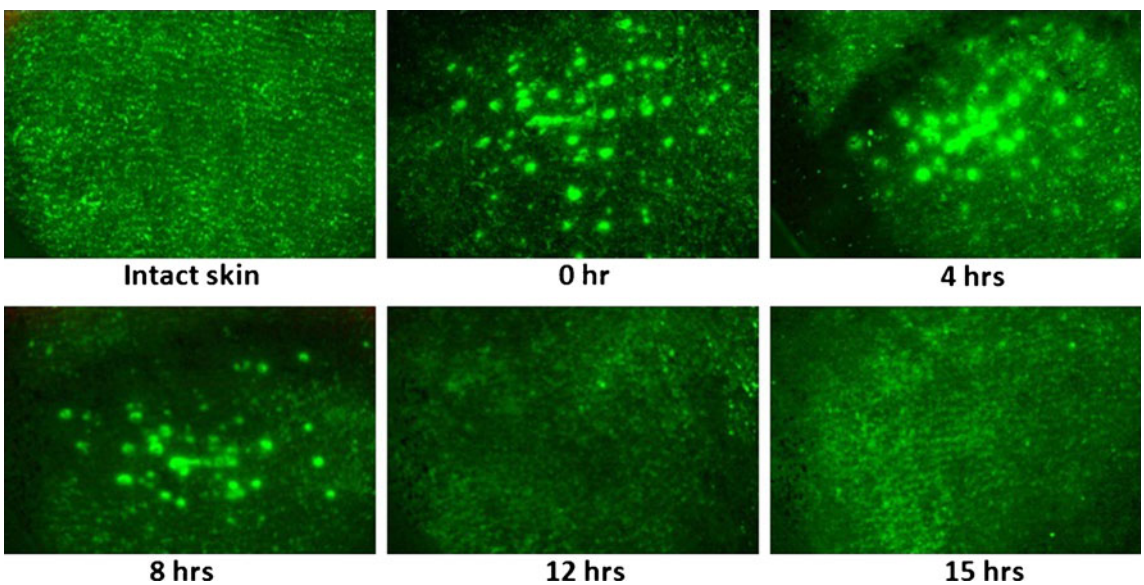

Fig. 10. Calcein imaging to study closure of pores created by 370 μm sized metal microneedles. Pores closed by 12 h, *in vivo*, indicating the reversible nature of skin microporation

studies with all three models of the DR series in separated epidermis and reported that immediately following microporation, microchannels had a pore size of 75, 125, and 180 μm for 150, 500, and 1,500 μm sized MN, as observed by SEM imaging. However, even in this *in vitro* condition, after 2 h of poration, pore sizes reduced dramatically to 15, 30, and 75 μm, respectively. Even though they speculate that the *in vitro* condition could have overestimated the pore size by 20%, the observed phenomenon indicates the significance of the role of skin's elasticity in resealing (25). The role of skin's elasticity and other biomechanical properties can perhaps be directly investigated with new emerging techniques such as OCT which enables direct *in vivo* imaging of the microporation process (26). It should also be noted that age, skin site, and application pressure will also play significant roles in pore closure kinetics.

Once the pore closure pattern has been established for a particular type of microneedles, if desired, pore closure can be further delayed by applying occlusive conditions. Occlusion in general has been known to delay barrier recovery (27–30). Hence, when clubbed with microneedle technology, it can result in a prolonged therapeutic window. In our previous studies, application of a water vapor-impermeable plastic film or a solution has been shown to decrease the rate of skin healing in soluble microneedles treated skin which delayed pore closure for up to 72 h (24). Gupta *et al*. have also reported that occlusion delayed pore closure in microneedle treated skin for up to 16–22 h (31). Alternatively, application of agents such as cox-inhibitors has also been reported to prolong pore closure for up to 7 days in guinea pigs (32). This appealing flexible nature of microneedle technology has prominent implications for drug delivery as it offers the possibility of a multi-day wear patch which is effective enough to deliver drugs over a period of days and at the same time safe enough due to the reversible nature of microchannels which avoids any related infection and irritation issues. Microneedle technology can therefore be customized as required to broaden the scope of delivery for prolonged periods of time.

Overall, the DermaRoller® offers a comparatively faster and reversible method than some other chemical and physical enhancement techniques and is highly patient and physician compliant. The stainless steel microneedles allow for multiple applications times (up to 100 times) when proper precautions are taken (16). In addition, it has also been reported that needling triggers release of growth factors and collagen induction which could play a synergistic role with the therapy, in some cases. However, this may not be desired for other treatment conditions and care much be taken to counteract these processes, such as application of agents which may delay or inhibit collagen induction. More recently, the Derma-Stamp™ was also introduced which has lesser number of microneedles and is more suitable for treatment of small, localized areas. It can also be effectively used for delivering vaccines by coating the vaccine formulation onto the defined set of stainless steel microneedles.

CONCLUSIONS

Our pursuit for simple and effective treatments and devices for several cosmetic and therapeutic applications has been a continual process. Microneedles offer a simple, reproducible, and effective means for breaching the stratum corneum barrier which allows for topical and transdermal delivery of hydrophilic molecules. The DermaRoller® device with metal microneedles is an easy to use handheld device which effectively creates microchannels and may provide an alternate means for skin microporation. The created microchannels are reversible in nature and close within a few hours of microporation; the time frame being dependent on the length of microneedles. This reversible nature of microchannels is very advantageous for controlled delivery of cosmetic agents/therapeutic compounds.

REFERENCES

1. Wermeling DP, Banks SL, Hudson DA, Gill HS, Gupta J, Prausnitz MR, *et al*. Microneedles permit transdermal delivery of a skin-impermeant medication to humans. Proc Natl Acad Sci U S A. 2008;105(6):2058–63.
2. Guy RH, Kalia YN, Delgado-Charro MB, Merino V, Lopez A, Marro D. Iontophoresis: electrorepulsion and electroosmosis. J Control Release. 2000;64(1–3):129–32.
3. Kalia YN, Naik A, Garrison J, Guy RH. Iontophoretic drug delivery. Advanced drug delivery reviews. 2004;56(5):619–58.
4. Lee JW, Park JH, Prausnitz MR. Dissolving microneedles for transdermal drug delivery. Biomaterials. 2008;29(13):2113–4.
5. Mitragotri S, Blankschtein D, Langer R. Ultrasound-mediated transdermal protein delivery. Science. 1995;269(5225):850–3.
6. Paliwal S, Mitragotri S. Ultrasound-induced cavitation: applications in drug and gene delivery. Expert opinion on drug delivery. 2006;3(6):713–26.
7. Prausnitz MR. Microneedles for transdermal drug delivery. Adv Drug Deliv Rev. 2004;56(5):581–7.
8. Prausnitz MR, Bose VG, Langer R, Weaver JC. Electroporation of mammalian skin: a mechanism to enhance transdermal drug delivery. Proc Natl Acad Sci U S A. 1993;90(22):10504–8.
9. Vemulapalli V, Yang Y, Friden PM, Banga AK. Synergistic effect of iontophoresis and soluble microneedles for transdermal delivery of methotrexate. J Pharm Pharmacol. 2008;60(1):27–33.
10. Banga AK. Transdermal and intradermal delivery of therapeutic agents: application of physical technologies. Boca Raton: CRC; 2011.
11. Kaushik S, Hord AH, Denson DD, McAllister DV, Smitra S, Allen MG, *et al*. Lack of pain associated with microfabricated microneedles. Anesth Analg. 2001;92(2):502–4.
12. Haq MI, Smith E, John DN, Kalavala M, Edwards C, Anstey A, *et al*. Clinical administration of microneedles: skin puncture, pain and sensation. Biomed Microdevices. 2009;11(1):35–47.
13. Gill HS, Denson DD, Burris BA, Prausnitz MR. Effect of microneedle design on pain in human volunteers. Clin J Pain. 2008;24(7):585–94.
14. Donnelly RF, Singh TR, Tunney MM, Morrow DI, McCarron PA, O'Mahony C, *et al*. Microneedle arrays allow lower microbial penetration than hypodermic needles in vitro. Pharm Res. 2009;26(11):2513–2.
15. Birchall JC, Clemo R, Anstey A, John DN. Microneedles in clinical practice—an exploratory study into the opinions of healthcare professionals and the public. Pharm Res. 2011;28(1):95–106.
16. Doddaballapur S. Microneedling with DermaRoller. J Cutan Aesthet Surg. 2009;2(2):110–1.
17. Majid I. Microneedling therapy in atrophic facial scars: an objective assessment. J Cutan Aesthet Surg. 2009;2(1):26–30.
18. Fabbrocini G, Fardella N, Monfrecola A, Proietti I, Innocenzi D. Acne scarring treatment using skin needling. Clin Exp Dermatol. 2009;34(8):874–9.
19. Leheta T, El Tawdy A, Abdel Hay R, Farid S. Percutaneous collagen induction versus full-concentration trichloroacetic acid in the treatment of atrophic acne scars. Dermatol Surg. 2011;37(2):207–16.
20. Henry S, McAllister DV, Allen MG, Prausnitz MR. Microfabricated microneedles: a novel approach to transdermal drug delivery. J Pharm Sci. 1998;87(8):922–5.
21. Kolli CS, Banga AK. Characterization of solid maltose microneedles and their use for transdermal delivery. Pharm Res. 2008;25(1):104–13.

22. Uhoda E, Pierard-Franchimont C, Debatisse B, Wang X, Pierard G. Repair kinetics of the stratum corneum under repeated insults. Exog Dermatol. 2004;3(1):7–11.
23. Li G, Badkar A, Nema S, Kolli CS, Banga AK. In vitro transdermal delivery of therapeutic antibodies using maltose microneedles. Int J Pharm. 2009;368(1–2):109–15.
24. Kalluri H, Banga AK. Formation and closure of microchannels in skin following microporation. Pharm Res. 2011;28(1):82–94.
25. Badran MM, Kuntsche J, Fahr A. Skin penetration enhancement by a microneedle device (Dermaroller) in vitro: dependency on needle size and applied formulation. Eur J Pharm Sci. 2009;36(4–5):511–23.
26. Coulman SA, Birchall JC, Alex A, Pearton M, Hofer B, O'Mahony C, *et al*. In vivo, in situ imaging of microneedle insertion into the skin of human volunteers using optical coherence tomography. Pharm Res. 2011;28(1):66–81.
27. Menon GK, Feingold KR, Elias PM. Lamellar body secretory response to barrier disruption. J Invest Dermatol. 1992;98 (3):279–89.
28. Ahn SK, Jiang SJ, Hwang SM, Choi EH, Lee JS, Lee SH. Functional and structural changes of the epidermal barrier induced by various types of insults in hairless mice. Arch Dermatol Res. 2001;293(6):308–18.
29. Kennish L, Reidenberg B. A review of the effect of occlusive dressings on lamellar bodies in the stratum corneum and relevance to transdermal absorption. Dermatol Online J. 2005;11(3):7.
30. Jiang S, Koo SW, Lee SH. The morphologic changes in lamellar bodies and intercorneocyte lipids after tape stripping and occlusion with a water vapor-impermeable membrane. Arch Dermatol Res. 1998;290(3):145–51.
31. Gupta J, Andrews S, Gill H, Prausnitz M. Kinetics of skin resealing after insertion of microneedles in human subjects. The 35th Annual Meeting and Exposition of the Controlled Release Society; July 19–22, 2008.
32. Banks SL, Paudel KS, Brogden NK, Loftin CD, Stinchcomb AL. Diclofenac enables prolonged delivery of naltrexone through microneedle-treated skin. Pharm Res. 2011;28:1211–9.